ISSN 1070-3632, Russian Journal of General Chemistry, 2017, Vol. 87, No. 6, pp. 1337–1350. © Pleiades Publishing, Ltd., 2017.
Original Russian Text © P.M. Pakhomov, S.D. Khizhnyak, I.N. Mezheumov, V.P. Galitsyn, 2015, published in Rossiiskii Khimicheskii Zhurnal, 2015, Vol. 59, No. 3, pp. 15–28.

Fabrication of High-Strength Fibers from Ultrahigh-Molecular-Weight Polyethylene

P. M. Pakhomov[a]*, S. D. Khizhnyak[a], I. N. Mezheumov[a], and V. P. Galitsyn[b]

[a] *Tver State University, Sadovyi per. 35, Tver, 170002 Russia*
**e-mail: pavel.pakhomov@mail.ru*

[b] *Research Institute of Synthetic Rubber (RISB), Moskovskoe sh. 157, Tver, 170032 Russia*

Received December 1, 2015

Abstract—Production of high-strength fibers from flexible-chain polymers having mechanical properties close to theoretically possible is one of the most important problems of physical chemistry and technology of polymers. Essential progress in this field has been achieved with the advent of gel spinning. Further enhancement of the mechanical properties of flexible chain polymers is possible only by complex investigations and, on their basis, goal-oriented formation of an optimal gel structure at all stages of the technological process. In this paper the structural transitions in ultrahigh-molecular-weight polyethylene (UHMWPE) in the course of gel spinning of high strength fibers were studied by optical spectroscopy, electron microscopy, X-ray diffraction, and differential scanning calorimetry. Special attention was devoted to such important stages of the gel spinning process as the liquid–gel transition and the transition of gel fibers into a highly oriented state. It was shown that the structure of thermoreversible UHMWPE gels can described in terms of a modified Keller model. According to this model, the nodes of the spatial gel network are lamellar microcrystallites 4-5 nm in thickness and 20 nm in lateral dimension. During orientation drawing of UHMWPE gel fibers, gradual straightening of molecular folds occurs, and the structure comprising crystallites on folded chains transforms to the structure composition fibrillar crystallites on straight chains. Investigation on a solvent-free technology of fabrication of high-strength film fibers from UHMWPE reactor powders (RPs) was initiated. The technology includes three stages: RP consolidation (compaction), fabrication of a monolithic film (monolithization), and orientation drawing of the monolithic film. A special cell for consolidation and monolithization is was developed. The effect of temperature and applied pressure on the consolidation and monolithization of the UHMWPE RP was studied. It was found that at ambient temperature and a pressure of 136 MPa the consolidation process is complete within 15 min. The optimal temperature range for the monolithization process is 135–140°C. First results of attempted orientation drawing of UHMWPE monolithic films are reported.

Keywords: reactor powder of high-molecular-weight polyethylene, gel spinning, solid-state spinning, high strength fibers and films, structural investigations

DOI: 10.1134/S1070363217060354

INTRODUCTION

The development of new and improvement of existing technologies of fabrication of polymers with extreme parameters, in particular, high strength parameters, is one the key challenges of technology of polymers. In late 1970s, Pennings, Smith, and Lemstra developed a gel-spinning technology for the fabrication of high-strength and high-modulus fibers from ultrahigh-molecular-weight polyethylene (UHMWPE). This technology allowed fabrication of fibers with record strengths (up to 3.0 GPa) and initial moduli (about 120 GPa), which were an order of magnitude higher compared with the respective parameters of commercial fibers obtained from flexible-chain polymers [1–3]. Even higher elastic and strength parameters of gel-spun fibers were attained in laboratory conditions (Table 1). As seen from the table, gel-spun UHMWPE fibers have the highest specific strength.

In view of the fact that UHMWPE fibers have not only a high strength, but also a complex of other unique properties, some counties (Germany, USA, and Japan) fairly rapidly (within 10–15 years) organized

Table 1. Elastic and strength parameters of the best poltmer and steel fibers [3]

Fiber	Strength, GPa	Elastic modulus, GPa	Density, g/cm^3	Specific density, GPa
UHMWPE (laboratory sample)	10.0	240	0.97	10.3
UHMWPE (Spectra)	3.5	125	0.97	3.6
Aramid (Armos)	5.0	150	1.43	3.5
Aromatic copolyester (Ekonol)	4.0	140	1.40	2.9
Polybenzothiazole (PBZ)	3.0	335	1.50	2.0
Steel	3.0	200	7.80	0.4

commercial production of such fibers. At present the annual global production of high-strength UHMWPE fibers is more than 12 ton and shows a stable tendency to increase.

However, the achieved strength parameters of UHMWPE fibers are no more than 10% the theoretically possible values and, therefore, much room still remains for raising the existing strength level. At present, gel spinning is the main technology that allows fabrication of ultrahigh-strength fibers from flexible-chain polymers. The technological process includes three major stages:

(1) preparation of the polymer solution;

(2) extrusion of the solution through a spinneret with the subsequent coagulation and formation of gel fibers;

(3) orientation drawing of gel fibers.

It should be noted that further enhancement of the mechanical properties of UHMWPE fibers is possible only via complex investigations and, on their basis, goal-oriented formation of an optimal gel structure and intermediate products at all stages of the technological process.

In this connection in the present work we set ourselves the task to perform a complex study of the structure of UHMWPE fibers at all stages of their fabrication, from the starting gel to the final highly oriented fibers, and correlate the structural transformations with mechanical properties.

The obvious disadvantage of the gel technology is that it makes use of environmentally hazardous solvents which are necessary to recycle; as a result, the cost of the final product is much increased [3]. Therefore, over the past years the attention of researchers and engineers has been focused on the development of the alternative, continuous solvent-free technology of the fabrication of ultrahigh-strength fibers from UHMWPE reactor powders (RPs) [3, 4].

At present the main problems of the latter technology, which call for scientific attention, include search for a UHMWPE reactor powder whose morphology would be suitable for the subsequent production of highly oriented materials by spinning technology [5, 6], as well as search for optimal conditions for all main stages of continuous solid-state spinning of the UHMWPE reactor powder (compaction, monolithization, orientation drawing) [7–9]. Solvent-free processing of UHMWPE reactor powders has found application in the fabrication of not only high-strength materials, but also robust membranes [10].

The process of solvent-free spinning of UHMWPE reactor powders has two important stages. The first is compaction of the RP under pressure at room temperature to obtain a mechanically strong workpieces (pellets). Compaction ensures a better contact between RP particles and remove air between them [9, 11]. The second important stage is monolithization, when the compacted RP is annealed under pressure to obtain a strong workpiece for the subsequent orientation drawing [8, 9, 11].

The important parameters of these two processes are the pressure applied to the RP, times of exposure of the RP to pressure, and monolithization temperature. These parameters strongly affect the strength characteristics of the films after compaction and monolithization, specifically, their ability for the subsequent orientation drawing. Therefore, one more goal of the present work was to determine optimal conditions (pressure, temperature, and time) for compaction and monolithization of UHMWPE reactor powders, as well as, in further work, for orientation drawing of monolithic films.

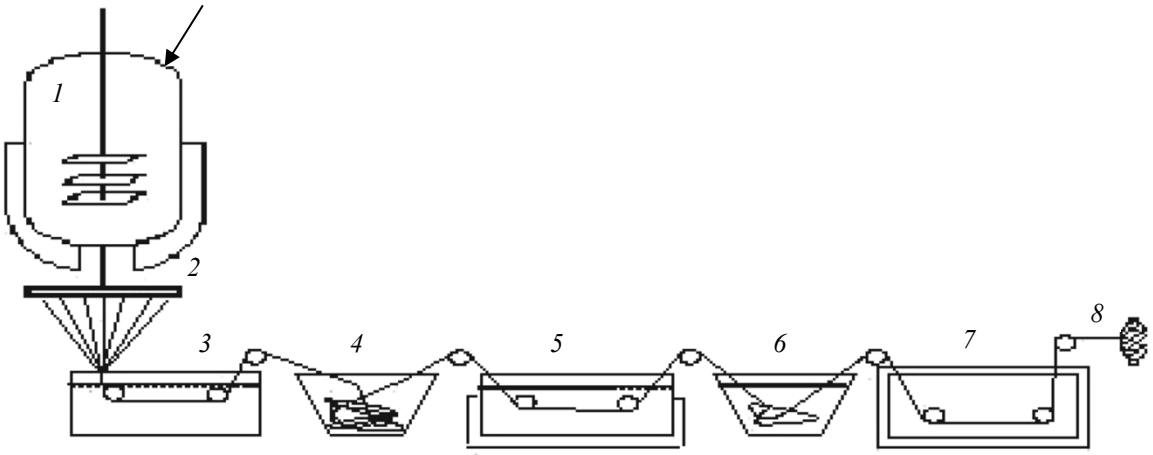

Fig. 1. Schematics of a pilot plant for gel spinning of high-strength UHMWPE yarns: (*1*) solution preparation reactor; (*2*) spinneret; (*3, 5*) baths for preliminary orientation drawing in a solvent medium at 70 and 125°C, respectively; (*4*) shrinkage bath; (*6*) solvent removal bath; (*7*) orientation drawing of the yarn in air at 145 °C; and (*8*) spun yarn bobbin.

Gel Spinning of High-Strength UHMWPE Fibers

As the object for study we used the UHMWPE reaction powder (MW from 1.7×10^6 to 14.2×10^6) synthesized at the Tomskneftekhim OAO and the Boreskov Institute of Catalysis, Siberian Branch, Russian Academy of Sciences, using a titanium–magnesium catalyst. Solutions and gels of UHMWPE with the polymer concentration of 5% were prepared as described in [12], using as solvents mineral oil, decaline, and *p*-xylene. Samples of UHMWPE fibers were obtained by gel spinning on a pilot plant [3], from a 3% spinning solution of the polymer in mineral oil (Fig. 1). The fiber comprising 240 filaments was subjected to orientation drawing in a solvent first at 70°C and then at 125°C until the draw ratio λ 30. Further on the oriented fiber was washed with hexane and additionally drawn in air at 145°C.

Mechanical testing of yarn fibers was performed on an Instron-1122 tensile-testing machine at a clamping length of 15 cm and a tensile speed of 0.05 m/min.

Wide-angle X-ray diffraction (WAXD) patterns were measured on a Stoe&Cie STADI P diffractometer and analyzed using the Debuy–Scherrer formula

$$L = K\lambda/\beta\cos\theta_{[200]}, \quad (1)$$

where L, nm, is the lateral dimension of the crystallite; K = 0.94; $\theta_{[200]}$, diffraction angle of the reflection [200]; and β, rad, half-width of the reflection [200]. Small-angle X-ray diffraction (SAXD) patterns were obtained using a Rigaku rotating anode X-ray source (CuK_α 1.54 Å).

The IR spectra of UHMWPE gels and fibers were recorded on a Bruker EQUINOX 55 FTIR spectrometer. The IR spectra of fibers were measured in polarized light. The molecular orientation of the polymer chains in crystalline regions was estimated by the formula

$$\langle\cos^2\upsilon\rangle = (2 - R)/(R + 2), \quad (2)$$

where υ is the angle between the axis of the molecular segment and the orientation axis of the fiber and R, dichroism of the IR band at 730 cm^{-1}, corresponding to rocking vibrations of the CH_2 groups in crystalline regions.

The Raman longitudinal acoustic mode (LAM) spectra were obtained on a Dilor XY800 triple-stage Raman microprobe. The Raman spectra were excited by monochromatic light (λ = 532 nm) from a Spectra Physics NdYVO laser source (100 W). The trans sequence length L and LAM frequency ν_L are related to each other by the equation

$$\nu_L = (2cL)^{-1}(E/\rho)^{1/2}, \quad (3)$$

where ν_L is the elastic rod acoustic resonant frequency; c, speed of light; ρ, density of the crystalline phase of the polymer; and E, elastic modulus of the straight chain. The LAM band shape reflects the distribution of straight chain segments (SCS) by lengths $F(L)$

$$F(L)\infty[1 - \exp(-hc\nu/kT)]\nu^2 I, \quad (4)$$

where T is the absolute temperature; I, LAM band intensity; k, Boltzman's constant; and h, Planck's constant. Differential scanning calorimetry (DSC) was performed on a Perkin−Elmer DSC-2 calorimeter.

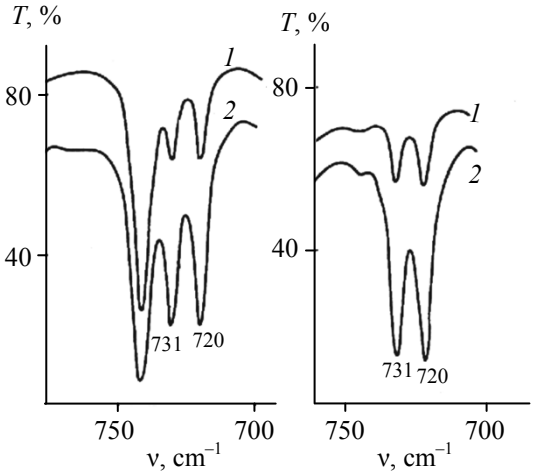

Fig. 2. IR transmission spectra of the UHMWPE gels obtained from (a) decaline and (b) *p*-xylene solutions with the polymer concentrations (*1*) 0.1 and (*2*) 1.5%. T = 20°C.

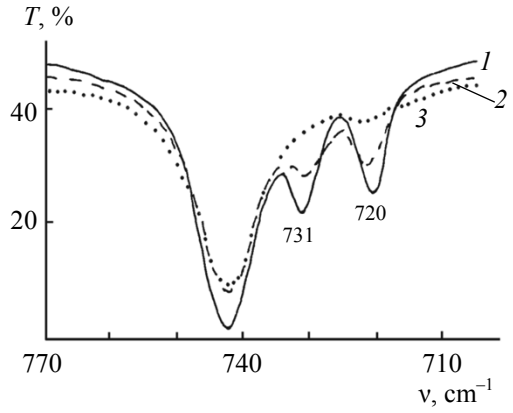

Fig. 3. IR transmission spectra of the UHMWPE gel in decaline at (*1*) 20, (*2*) 80, and (*3*) 90°C.

The surface morphology of fibers, films, and pellets was studied by scanning electron microscopy (SEM) on a Jeol 6300 LV microscope.

According to the IR spectral data in [12], UHMWPE gels contain a crystalline phase (Fig. 2). Direct evidence for this conclusion was provided by the observation of a "crystalline" doublet at 720 and 731 cm^{-1}. As the temperature was increased, the doublet decreased in intensity (Fig. 3) and disappeared completely at 90°C, when the gel dissolved [13]. If the solution was cooled down, the crystalline phase formed again, the IR spectrum reverted to the original one, and the solution transformed into a gel. Thus, UHMWPE gels are thermally reversible physical gels.

The gelation of the UHMWPE solution was also accompanied by a sharp increase of viscosity (by 3–4 orders of magnitude), which suggests formation of a continuous 3D polymer network, the nodes of which, according to the Keller model [14], are crystalline regions (microcrystallites) [15].

Analysis of the Raman spectra and DSC curves [15–18] showed that the nodes of the 3D network in the gel are formed by crystallites on folded chains (lamellar microcrystallites). Figure 4a depicts the Raman spectra of UHMWPE gels in different solvents. As seen, the low-frequency region displays a broad LAM band. This fact suggests the presence of regular macromolecular regions in the material. The SCS distributions by length $F(L)$, calculated from the Raman spectra, are shown in Fig. 4b. The most probable length of an SCS (L_s) corresponds to the LAM band maximum. It was found that L is almost independent both on the concentration of the solution and on the molecular weight of the polymer. The fact that L is

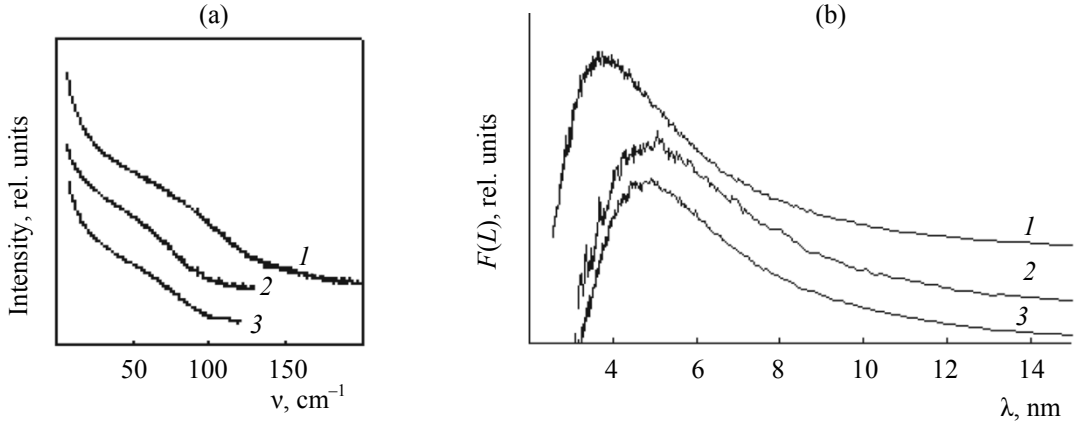

Fig. 4. (a) Raman spectra and (b) length distributions of straight chain segments for the UHMWPE gels (c = 2.5%) in (*1*) *p*-xylene, (*2*) mineral oil, and (*3*) decaline.

insensitive to the concentration of the solution suggests that the SCSs in the gels rather than being isolated trans sequences are incorporated in crystalline regions, the dimensions of which are defined by the thermodynamic conditions of their formation. Therefore, we can consider that the L_s value coincides with the average thickness of microcrystallites. The L_s value proved to be the most sensitive to the solvent. Thus, the L_s values for the gels obtained from solutions in *p*-xylene, decaline, and mineral oil were 3.7, 5.0, and 5.2 nm, respectively.

According to our X-ray diffraction data [19], the lateral dimensions of the crystalline nodes (18–20 nm) are larger than longitudinal. Thus, these data provide evidence for the Keller model [14] for thermally reversible gels.

Figure 5 shows how the mechanical characteristics of multifilament fibers changed in the course of orientation drawing [20]. As seen, UHMWPE fibers were drawn to high draw ratios (~80), and their tensile strength and elastic modulus reached very high values (~3.7 and ~150 GPa, respectively). It should also be noted that the strength of the fiber strongly increased from the very beginning of drawing, while the modulus, only starting with the draw ratio 10 or higher. No correlation between crystallite orientation and elastic modulus was also observed [13].

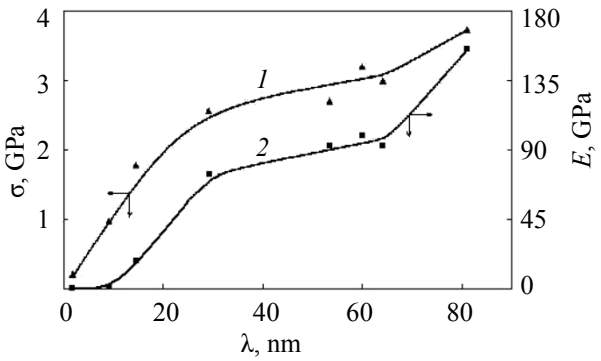

Fig. 5. Dependences of the (*1*) strength and (*2*) elastic modulus of multifilament UHMWPE fibers on draw ratio.

The changes in the morphology of UHMWPE fibers in the course of drawing are shown in Fig. 6. As seen, if at the first stage of drawing there are a lot of cross-links between fiber microfibrils (Fig. 6a), at the

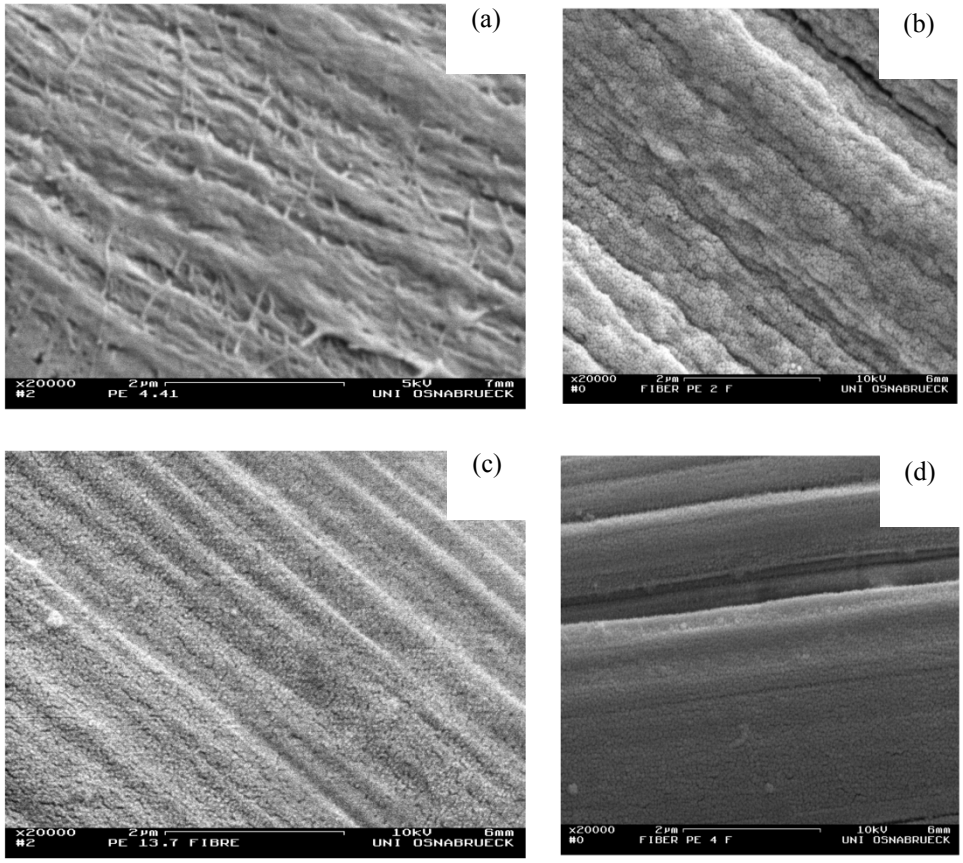

Fig. 6. SEM images of UHMWPE fibers with the draw ratios (a) 4.4, (b) 9.0, (c) 13.7, and (d) 74.9.

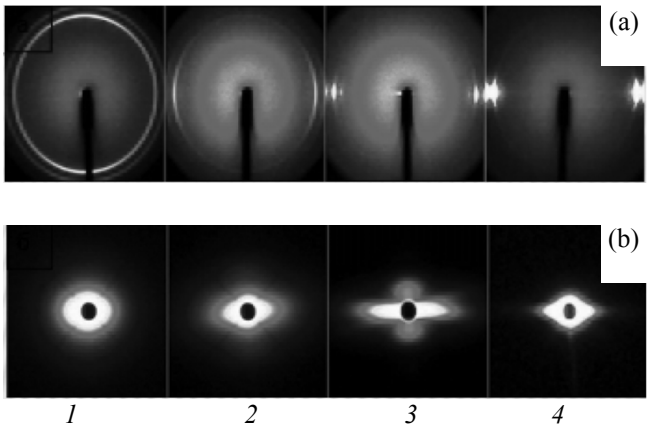

Fig. 7. (a) WAXD and (b) SAXD images of vertically aligned UHMWPE fibers. Draw ratio: (*1*) 1.7, (*2*) 9.0, (*3*) 15.0, and (*4*) 75.0.

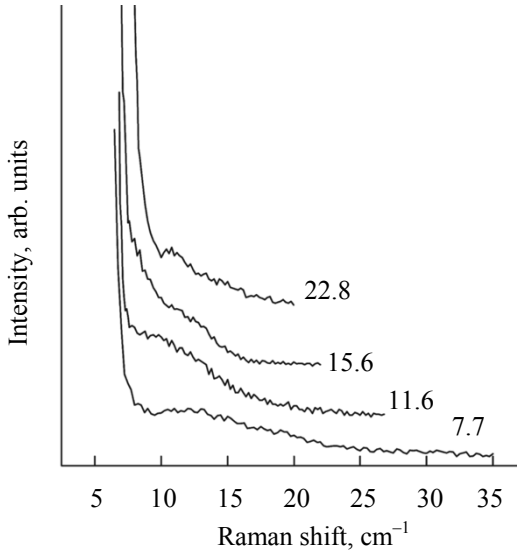

Fig. 8. Low-frequency Raman spectra in the LAM range for UHMWPE fibers with different draw ratios.

final stage (Fig. 6g) microfibrils are mutually oriented and have a smooth surface.

Figure 7 shows the WAXD and SAXD patterns of UHMWPE fibers with different draw ratios [21]. As seen, with increasing draw ratio, the crystallite orientation in microfibrils becomes much higher, and the molecular chains in crystallites are packed into an orthorhombic lattice. At the first stages of orientation drawing (the samples with λ = 1.9, 9.0, and 18), a microfibrillar structure is formed, as evidenced by an increase in equatorial scattering (Fig. 7b). With the sample with λ = 15, we also observed a well-defined meridional scattering, which suggests the presence of a large period or alternating crystalline and amorphous regions inside microfibrils. At high draw ratios (λ = 76) the meridional reflex disappeared, probably, because of an equalization of the densities of the crystalline and amorphous regions.

The Raman LAM spectra of the of UHMWPE fibers with different λ values are shown in Fig. 8, and the $F(L)$ functions calculated by Eq. (4) are presented in Fig. 9 [13, 22]. The maxima in the $F(L)$ curves in Fig. 9 correspond to the average L_{SCS} value. In a general case:

$$L_{SCS} = L_c + L_{RAP}, \quad (5)$$

where L_C is the longitudinal dimension of the crystallite, L_{RAP}, length of the rigid amorphous phase in the transition zone between the crystalline and amorphous phases. In the case of a poorly oriented UHMWPE fiber with λ = 7.7, like in the case of the gel, $L_{SCS} \approx L_C$ and $L_{RAP} \approx 0$. Therewith, L_C is independent on the draw ratio of the fibers obtained at given temperature conditions. Consequently, we can conclude that the shift of the $F(L)$ maximum to larger L values with increasing λ (Fig. 9) is associated with straightening of fords on the crystallite surface. This process forms a rigid amorphous phase, which immediately increases the elastic modulus of the fiber (Fig. 5).

At $\lambda \geq 15.6$ the $F(L)$ function becomes bimodal (Fig. 9c). The position of the second peak at $L \approx 35$ nm corresponds to about $2L_C \approx 32$ nm, where $L_C \approx 16$ nm for the sample with λ = 7.7 (Fig. 9a). This result means that the bimodal SCS distribution is explained by the appearance of straight chains bridging two neighboring crystallites. Such a qualitative change in the SCS distribution has almost no effect on the quasilinear increase in the elastic modulus at $\lambda > 7.7$. In view of the unique correlation of the elastic modulus with λ, the latter fact implies that the rearrangement of the rigid amorphous phase does not disturb the "morphologic continuity" of the drawing process.

Thus, the increasing "crystalline continuity" along the fiber axis is associated with straightening of fords on the lamellar crystallite surface. We first observed the process of chain straightening near the crystallite surface in our experiments on isothermal stress

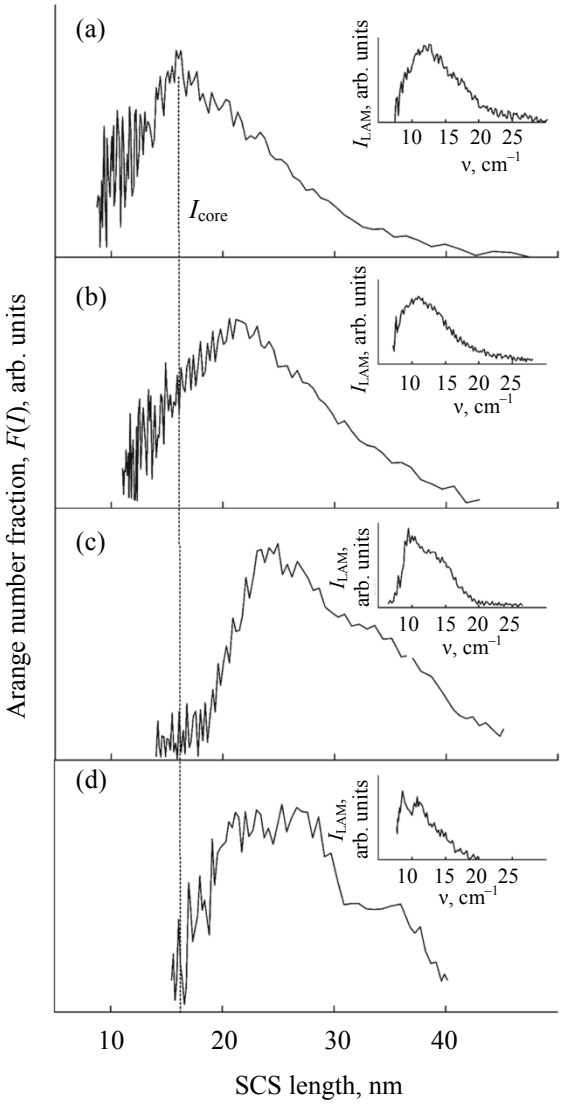

Fig. 9. SCS distribution functions $F(L)$ for UHMWPE fibers with different draw ratios: (a) 7.7, (b) 7.7, (c) 15.6, and (d) 22.8.

relaxation [23]. The appearance of RAP with simultaneous increase in the elastic modulus provide evidence in favor of the "bridge model" of the structure of highly oriented fibers [23, 24], proposed to explain paradoxical XRD data, when the longitudinal crystallite size was larger than the large period. According to this model, "long crystals" formed by straightened chain segments bridging folded crystallites. The appearance of bimodality on the $F(L)$ curve (Fig. 9c) points to the formation in the amorphous phase of straight chains bridging neighboring crystallites. Such chains increase in number on further drawing, and they form the PAP or crystalline bridges (Fig. 10).

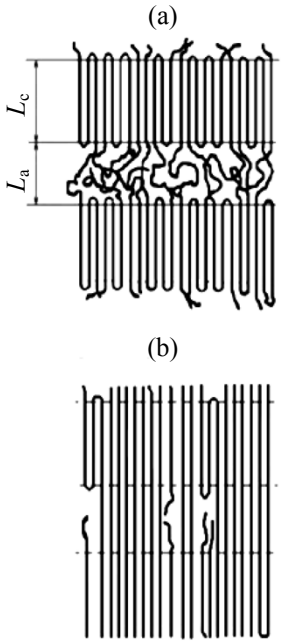

Fig. 10. Structural models of (a) low- and (b) high-oriented UHMWPE fibers.

Consequently, in the course of orientation drawing of UHMWPE gel fibers the structure comprising crystallites on folded chains gradually transforms into the structure comprising defect fibrillar crystallites on straight chains (Fig. 10). The decrease in the quantity of defect amorphous segments inevitably increases the strength of the fiber. Having established the effect of the morphology of the starting reactor powder on the mechanical properties of the final fiber [25] and determined the optimal conditions of fiber formation and drawing at all stages of the technological process, we could obtain multifilament UHMWPE fibers with the tensile strength of 4 GPa.

Thus, our study showed that the structure of thermally reversible UHMWPE gels is adequately described by the Keller model. According to this model, the lamellar microcrystallites, ~4–5 nm in thickness and ~20 nm in lateral dimension, form nodes of the spatial gel network. Orientation drawing straightens folds in the lamellar crystallite, increases crystalline continuity along the fiber axis, and, as a result, considerably enhances the elastic and strength characteristics of the resulting fibers.

Compaction and Monolithization of UHMWPE Reactor Powders

The objects for study were the UHMWPE reactor powders with the viscosity-average molecular weights

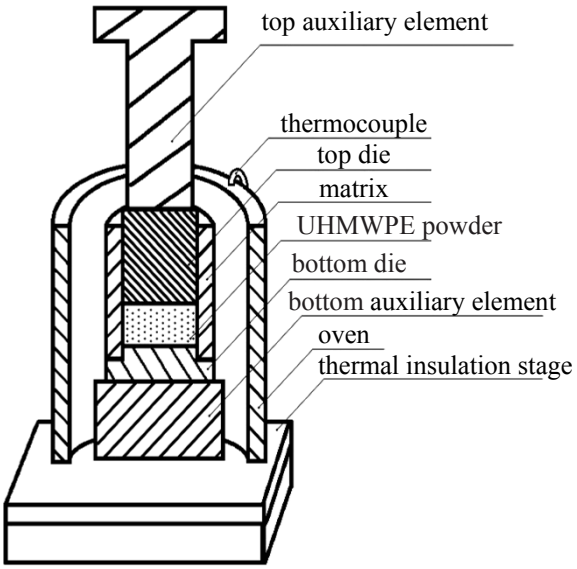

Fig. 11. Heated press form with a thermally insulated bottom.

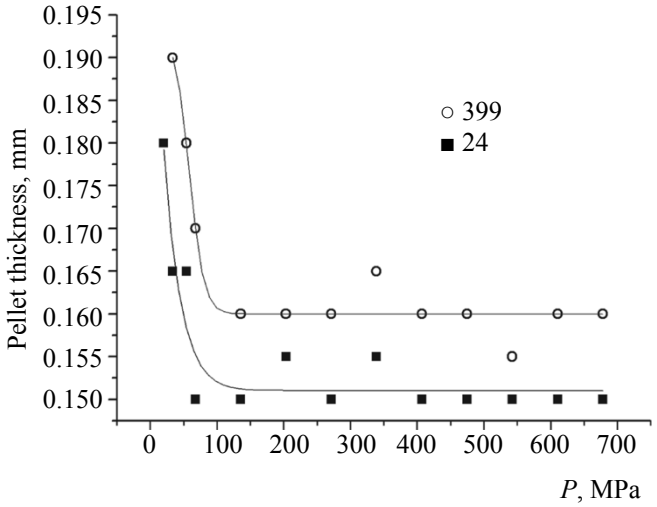

Fig. 12. Dependences of the pellet thickness at the center on the applied pressure. Pressing time 15 min, room temperature.

Mη of 4.3×10^6 g/mol (batch no. 399) and 3.7×10^6 g/mol (batch no. 24) synthesized at the Boreskov Institute of Catalysis, Siberian Brach, Russian Academy of Sciences, using the titanium–magnesium catalysts TS-71 (batch no. 399) and TS-115 (batch no. 24). It should be noted that the fibers fabricated by gel spinning from the RP from batch no. 399 had the highest tensile strength (σ = 4.0 GPa) [3], whereas the fibers fabricated from the RP from batch no. 24 had lower strength characteristics. Compaction of the UHMWPE reactor powders was performed on a PIKE Crush IR hydraulic press for making pellets. The RP sample (0.0175 g) was loaded to a press form (ram stroke diameter 13 mm), and pellets were formed under external pressure varied from 20.4 to 678.2 MPa for 8 or 15 min at room temperature. The dimensions of the resulting pellets (thickness at the center and at the edge) were measured with a dial gauge with an accuracy of ±0.01 mm.

The monolithization process was studied using the UHMWPE pellets compacted at room temperature for 15 min under a constant pressure of 135.6 MPa in a specially designed press form (Fig. 11) with the ram stroke diameter of 30 mm for 30 min in the temperature range 20–175°C under a constant pressure of 30 MPa. After monolithization was complete and the press form cooled down, the ready pellet or film was taken out, and its thickness at the center was measured.

The average particle size of the UHMWPE reactor powders on the pellet or film surface was calculated by the Image Pro program.

The crystallinity of the samples obtained by the consecutive compaction and monolithization of UHMWPE reactor powders was estimated by FTIR spectroscopy on a Bruker Equinox 55 spectrometer by the intensity ratio of the bands at 720 and 730 cm^{-1} [26]:

$$\alpha = \frac{D_{730}}{D_{720}}, \qquad (6)$$

where D_{730} is the optical density of the absorption band related to the crystalline phase of the polymer and D_{720}, optical density of the absorption band related to the amorphous and crystalline phase of the polymer. The optimal conditions of monolithization were determined by IR spectroscopy by our previously developed procedure which involved estimation of scattered radiation from the sample [27]. The compaction of UHMWPE reactor powders at room temperature was performed for 8 or 15 min in the pressure range 34.2–678.2 MPa.

Figure 12 shows the estimated central thicknesses of compacted pellets fabricated from the RPs from batch nos. 399 and 24.

It was found that at the initial pressure ranging from 34.2 to 67.8 MPa the pellet thickness sharply decreased with increasing pressure. However, at pressures

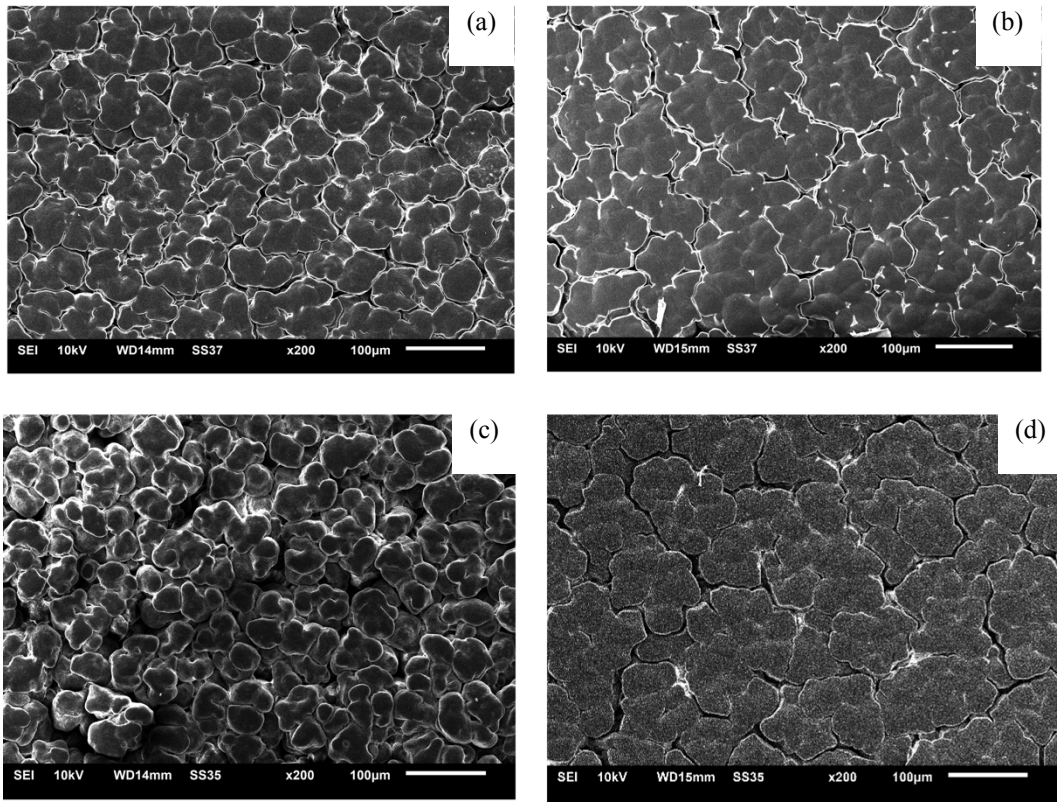

Fig. 13. SEM images of the pellets fabricated from the UHMWPE reactor powders from batch nos. (a, b) 399 and (c, d) 24 at different pressures, MPa: (a, c) 54.3 and (b, d) 407.0.

ranging from 67.8 to 678.2 MPa the pellet thickness changed only slightly. The thickness of the pellets obtained from different batches of the RP varied in parallel with applied pressure. It should also be noted that the pellet thickness only slightly varied as the compaction time was increased from 8 to 15 min over the entire pressure range studied. This fact allows us to conclude that the time sufficient to complete compaction of the UHMWPE reactor powder is 8 min or more.

Analysis of the resulting data shows that the thickness of the UHMWPE pellets formed at low pressures (<67.8 MPa) much decreases due to a closer packing the starting RP particles and their plastic deformation [9].

Further increase of the pressure (above 135.6 MPa) does considerably affect the free volume inside the pellet and its dimensions, which is explained by the elasticity of the RP particles and the whole pellets. Therefore, we can conclude that the compaction of the UHMWPE reactor powder at room temperature is complete at 136.0 MPa.

The micrographs of the compacted pellets show that the packing of RP particles gets closer as the applied pressure increases. Thus, the pellets formed at low pressure (Fig. 13a and 13b) have a fairly large free volume, especially in the case of the RP from batch no. 24, but those formed at higher pressures (Figs. 13b and 13d) contain closely packed RP particles. Moreover, the RP particles deform (flatten) under high pressure.

Thus, at the compaction stage RP particles come in contact with each other. As a result, the packed density of the powder increases and its free volume decreases. After the particles have packed sufficiently tightly, they start to undergo plastic deformation (at pressures higher than 30–60 MPa), which leads to further compacting of the RP pellet. At pressures higher than 136 MPa, the UHMWPE reactor powders begin to exhibit elastic behavior, and the pellet thickness no longer changes (Fig. 12). The micrographs displayed an almost complete plastic deformation, while the average size of compacted RP particles almost did not vary at high pressures. It was also found that the compaction of the UHMWPE reaction powder has an essential impact of the RP structure [5].

To study the monolithization process of the UHMWPE reaction powder in a hot pellet press

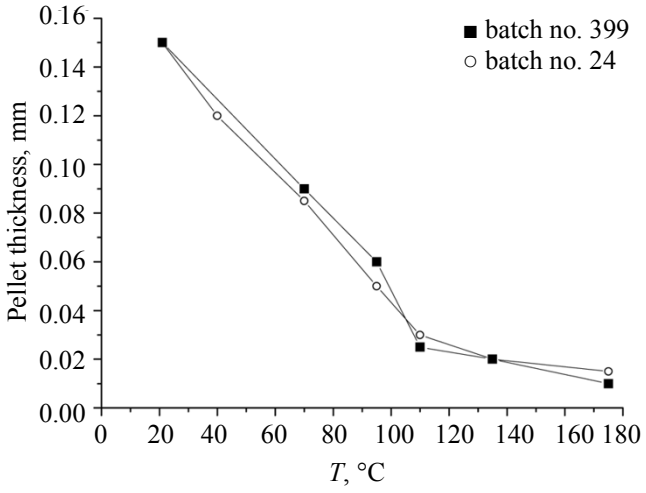

Fig. 14. Temperature dependences of the thickness of the monolithic pellets fabricated from the UHMWPE reactor powders from batch nos. 24 and 399. Pressure 30 MPa, monolithization time 30 min.

(Fig. 11), we used the pellets compacted under optimal conditions: at the pressure 136.0 MPa and the compaction time 15 min. The dependence of film thickness on monolithization temperature is shown in Fig. 14.

As seen, in the temperature range 20–100°C, the pellet thickness strongly decreases with increasing temperature. However, on heating above 110°C the pellet thickness varies only slightly. Such results allow us to conclude that the optimal monolithization temperature is ~135–140°C. Higher temperatures are undesirable in view of the sharp intensification of destructive processes [3]. The micrographs in Fig. 15 show that the packing of RP particles becomes closer with temperature. At 75°C the interparticle contacts in the pellet obtained from the RP from batch no. 24 are much less close (as evidenced by the greater number of interfaces) than in that obtained from the RP from batch no. 399. The same situation is observed at all the other temperatures. In the sample obtained from the RP from batch no. 399, an almost monolithic film is formed at 135°C (Fig. 15b). At the same time, in the sample obtained from the RP from batch no. 24, quite a few interfaces between subparticles are still observed (Fig. 15d). To determine an optimal monolithization temperature for UHMWPE reactor powder, we measured the IR transmission spectra of the films obtained by sintering pellets from both RP batches in a heated press form in the temperature range 40–175°C (Fig. 16). It was found that the transmittance of the samples obtained at low temperatures (40–70°C) was

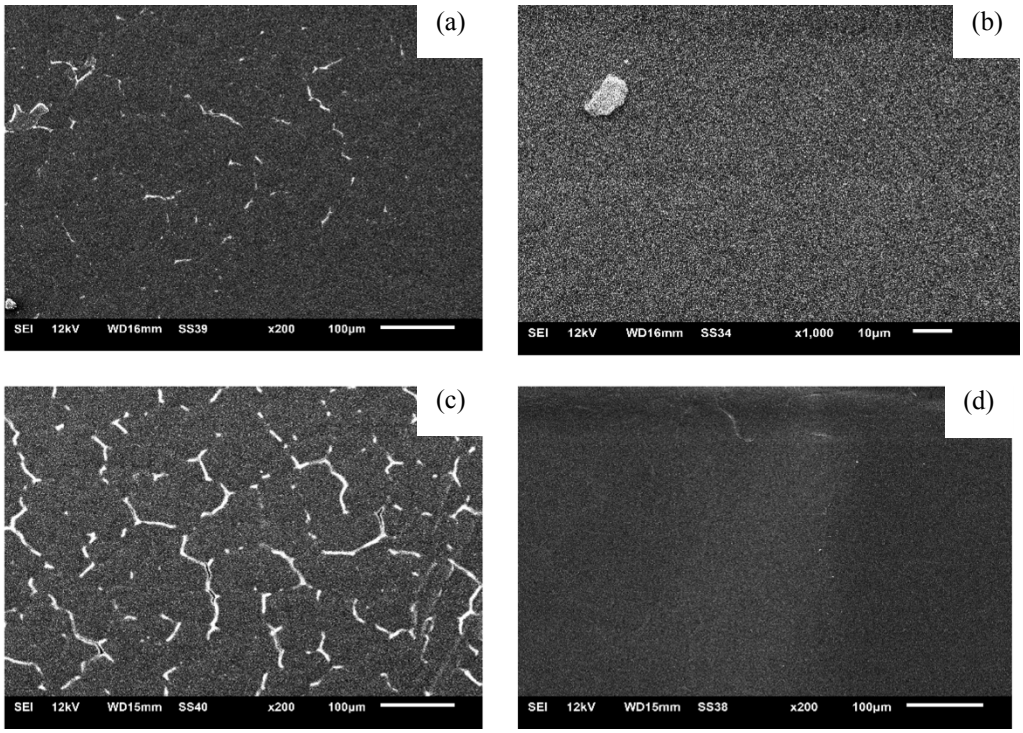

Fig. 15. Surface SEM images of the monolithic pellets fabricated from the UHMWPE reactor powders from batch nos. (a, b) 399 and (c, d) 24 at different temperatures, °C: (a, c) 75 and (b, d) 135.

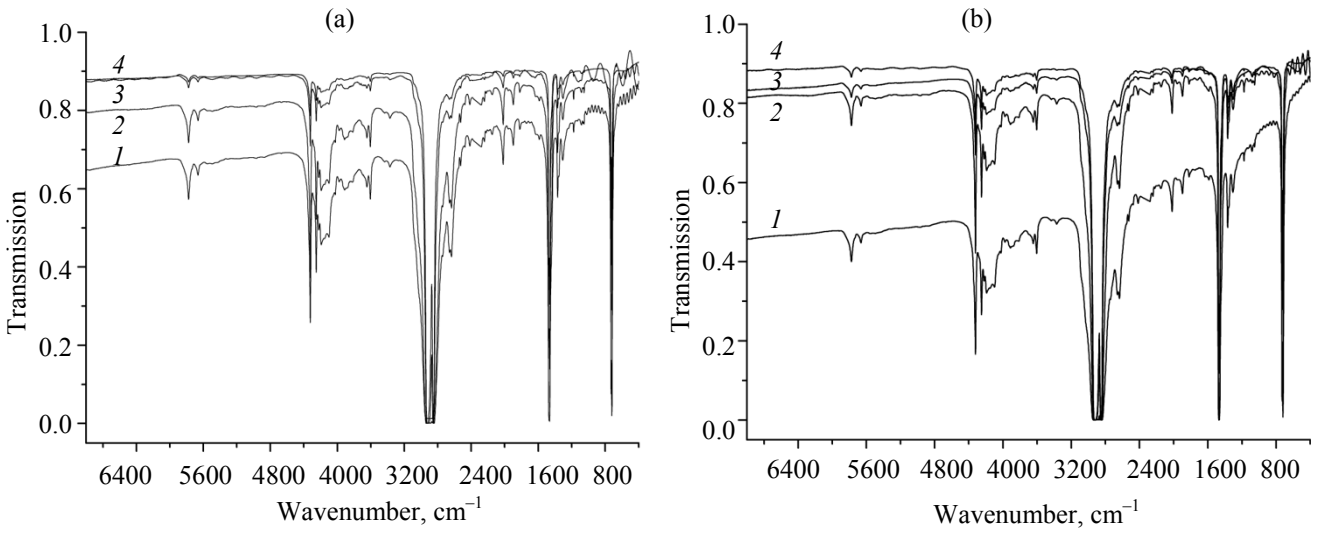

Fig. 16. IR transmission spectra of the compacted pellets fabricated from the UHMWPE reactor powders from batch nos. (a) 399 and (b) 24 and monolithized at different temperatures, °C: (a): (*1*) 70, (*2*) 95, (*3*) 135, and (*4*) 175; (b): (*1*) 40, (*2*) 95, (*3*) 135, and (*4*) 175. Pressure 30 MPa, monolithization time 30 min.

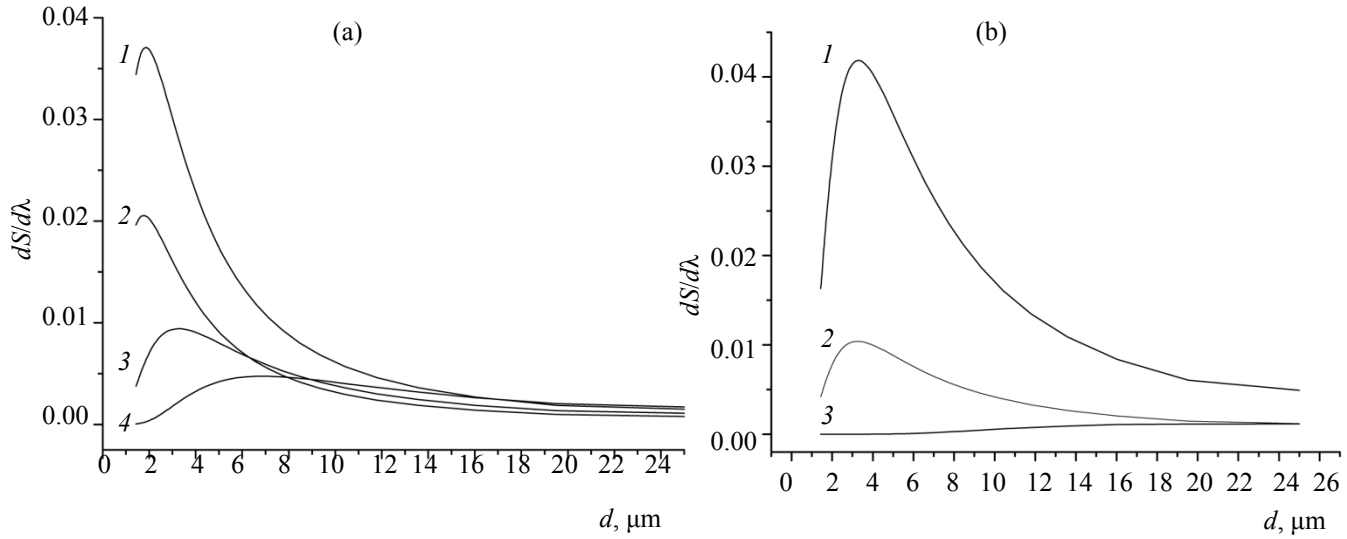

Fig. 17. Size distributions of scattering particles in the films fabricated by the monolithization of compacted pellets from batch no. (a) 399 and (b) 24 UHMWPE reactor powders at different temperatures, °C: (a): (*1*) 70, (*2*) 95, (*3*) 135, and (*4*) 175°C; (b): (*1*) 70, (*2*) 110, and (*3*) 175.

lower than those obtained at 135 and 175°C over the entire frequency range. This is first of all explained by the fact that the pellets obtained at high temperatures are thinner and contain less scattering centers. In view of the only slight variation of the IR spectra of the pellets from batch no. 399 reactor powders, obtained at high temperatures, we concluded that the optimal monolithization temperature is 135–140°C.

Based on the data in [27], from the IR spectra in Fig. 16 we could estimate the average size of scattering particles and also their size distribution. The presence of scattering particles in the monolithic film, i.e. its nonuniformity, may strongly affect the final mechanical properties of the UHMWPE film fiber. Figure 17 shows the size distribution curves of scattering particles in the monolithic UHMWPE films, calculated from the IR spectra (Fig. 16). Analysis of the resulting data shows that the average diameter of scattering particles is directly related, while their concentration is inversely related to monolithization temperature.

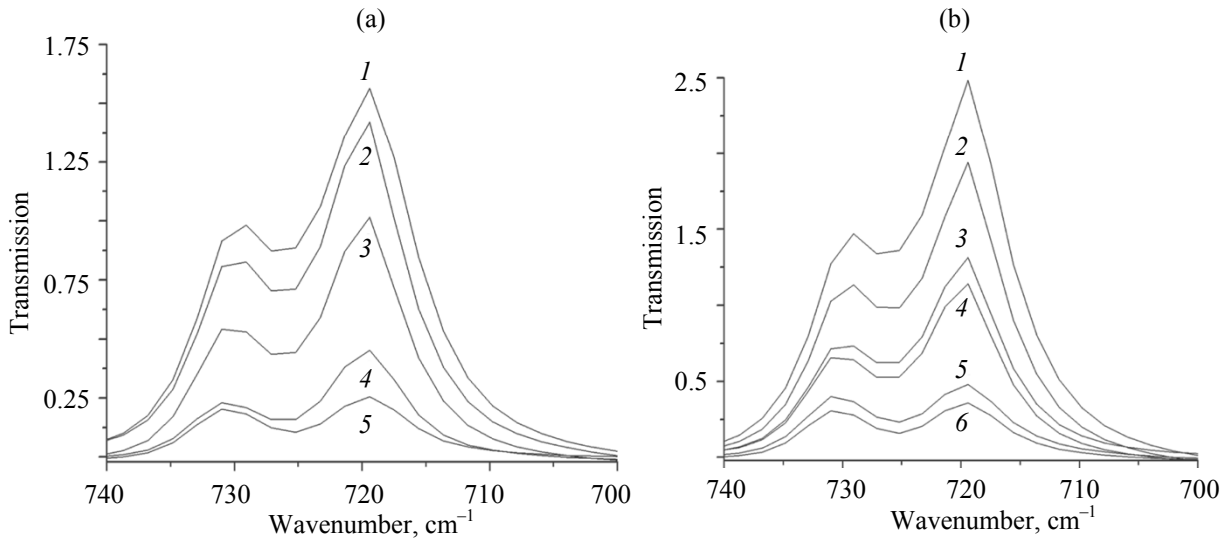

Fig. 18. Behavior of the crystalline doublet 720/730 cm–1 in the IR spectra of the monolithic films fabricated from compacted pellets from batch no. (a) 399 and (b) 24 UHMWPE reactor powders at different temperatures, °C: (a): (*1*) 70, (*2*) 95, (*3*) 110, (*4*) 135; and (*5*) 175; (b): (*1*) 40, (*2*) 70, (*3*) 96, (*4*) 110, (*5*) 135, and (*6*) 175.

Of interest is also the behavior of the crystallinity of the monolithic films with temperature. Figure 18 shows the behavior of the crystalline doublet 720/730 cm^{-1} depending on the temperature of monolithization of UHMWPE films.

As seen, the intensity of the doublet decreases with increasing monolithization temperature. This effect is explained by the fact that the film thickness strongly decreases as the monolithization temperature increases (Fig. 14). The degrees of crystallinity α for the monolithic UHMWPE films, estimated from the IR spectra (Fig. 18) by the above formula, are listed in Table 2. Analysis of the data in Table 2 shows that the degree of crystallinity decreases as the monolithization temperature is increased to 110°C.

Table 2. Degrees degree of crystallinity (α) of the UHMWPE films monolithized at different temperatures at a pressure of 30.0 MPa for 30 min

UHMWPE RP batch no. 399		UHMWPE RP batch no. 24	
T, °C	α	*T*, °C	α
65	0.62	40	0.61
70	0.63	60	0.62
95	0.59	70	0.60
110	0.56	95	0.57
135	0.70	110	0.58
175	0.81	135	0.84
		175	0.87

Such behavior is apparently explained by radical morphological and polymorphous transformations in the UHMWPE [3, 28]: individual RP particles form a homogeneous film and the monoclinic crystal phase transforms into orthorhombic. With the RPs from bath no. 399, this process is complete at 135–140°C. With further increase of temperature, the degree of crystallinity increases for both RP batches, but this result does not imply that the orientation drawing of such films will give the strongest fibers (if anything). Actually, films with the highest degree of crystallinity are more difficult to transform into highly oriented fibers. Moreover, further strengthening at high temperatures is prevented by the intensified thermal destruction. Consequently, the optimal monolithization temperature for the UHMWPE films fabricated from the RP from bathcn no. 399 is 135–140°C. The RP from batch no. 24 is no well compacted and monolithized under these condition compared to that from batch no. 399. Apparently, just the structural difference of the starting UHMWPE reactor powders explains the different mechanical characteristics of the final gel-spun fibers [3].

Thus, we determined optimal conditions (temperature, pressure, time) of the main stages (compaction and monolithization) of solvent-free gel spinning of UHMWPE reactor powders.

CONCLUSIONS

A complex of methods was used to study structural transformations at the main stages of gel spinning of UHMWPE fibers.

It was found that, in compliance with the Keller model, the nodes of the 3D gel network are formed by microcrystallites (~4-5 nm in thickness and ~20 nm in lateral size) on folded chains.

Evidence was obtained showing that in the course of orientation drawing of UHMWPE gel fibers the structure comprising crystallites on folded chains gradually transforms into the structure comprising crystallites on straight chains. The increase of the crystalline continuity along the axis of the fiber much enhances its elastic and strength characteristics.

A domestic technology of gel spinning of multifilament UHMWPE fibers with the tensile strength of 4 GPa was developed.

Optimal conditions (temperature, pressure, time) of the main stages (compaction and monolithization) of solvent-free gel spinning of high-strength film fibers from UHMWPE reactor powders.

ACKNOWLEDGMENTS

The work was funded by the Ministry of Education and Science of the Russian Federation through the State Contract for Scientific Research (project no. 4.1325.2014/K).

REFERENCES

1. Kalb, B. and Pennings, A.J., *Polym. Bull*., 1979, no. 1. p. 871.
2. Smith, P. and Lemstra, P.J., *Macromol. Chem*., 1979, vol. 180, p. 2983.
3. Pakhomov, P.M., Galitsyn, V.P., Khizhnyak, S.D., and Chmel', A.E., *Vysokoprochnye i vysokomodul'nye polimernye volokna* (High-Strength and High-Modulus Polymer Fibers), Tver': Tver. Gos. Univ., 2012.
4. Joo, Y.L., Zhou, H., Lee, S.-G., Lee, H.-K., and Song, J.K., *J. Appl. Polym. Sci*., 2005, vol. 98, p. 718. doi 10.1002/app.22076
5. Sitnikova, V.E., Kotova, A.A., Galitsyn, V.P., Khizhnyak, S.D., and Pakhomov, P.M., *Fibre Chem.,* 2012, no. 6, p. 331. doi 10.1007/s10692-013-9457-5
6. Ivan'kova, E.M., Myasnikova, L.P., Marikhin, V.A., Baulin, A.A., and Volchek, B.Z., *J. Macromol. Sci. B*, 2001, vol. 40, no. 5. p. 813.
7. Aulov, V.A., Makarov S.V., Kuchkina, I.O., Panthyukhin, A.A., Akopyan, A.L., Ozerin, A.N., and Bakeev, N.F., *Polymer Sci., Ser. A*, 2001, vol. 43, no. 10, p. 1008.
8. Ozerin, A.N., Ivanchev, S.S., Chvalun, S.N., Aulov, V.A., Ivancheva, N.I., and Bakeev, N.F., *Polymer Sci., Ser. A*, 2012, vol. 54, no. 12, p. 950. doi 10.1134/S0965545X12100033
9. Pakhomov, P.M., Pogudkina, A.A., Mezheumov, I.N., Khizhnyak, S.D., Ivanova, A.I., Grechishkin, R.M., and Galitsyn, V.P., *Fibre Chem*., 2014, vol. 46, no. 1, p. 5. doi 10.1007/s10692-014-9551-3
10. Uehara, H., Tamura, T., Hashidume, K., Tanaka, H., and Yamanobe, T., *J. Mater. Chem. A*, 2014, no. 2, p. 5252. doi 10.1039/C3TA15125E
11. Pogudkina, A.A., Mezheumov, I.N., Khizhnyak, S.D., Ivanova, A.I., Grechishkin, R.M., Galytsin. V.P., and Pakhomov, P.M., *Fiz. Khim. Polimerov*, *Tver: Tver. Gos. Univ*., 2013, no. 19, p. 75.
12. Pakhomov, P.M., Larionova, N.V., and Alekseev, V.G., *Vysokomol. Soedin., Ser. A*, 1995, vol. 37, no. 5, p. 892.
13. Pakhomov, P.M., Khizhnyak, S.D., Golikova, A.Yu., Galitsyn, V.P., and Chmel', A.E., *Polymer Sci., Ser. A*, 2005, vol. 47, no. 4, p. 389.
14. Keller, A., *Faraday Discuss*., 1995, vol. 101, p. 1. doi 10.1039/FD9950100001
15. Pakhomov, P.M.,, Chmel', A.E., Khizhnyak, S.D., and Galitsyn, V.P., *Dokl. Akad. Nauk*, 2002, vol. 386, no. 2, p. 220.
16. Kober, K., Khizhnyak, S., Pakhomov, P., and Tshmel, A., *J. Appl. Polym. Sci*., 1999, vol. 72, p. 1795. doi 10.1002/(SICI)1097-4628(19990624)72:13<1795::AID-APP15>3.0.CO;2-3
17. Pakhomov, P., Khizhnyak, S., Kober, K., and Tshmel, A., *Eur. Polym. J.,* 2001, vol. 37, p. 623.
18. Pakhomov, P.M., Khizhnyak, S.D., Galitsyn, V.P., Ruhl, E., Vasil'eva, V., and and Tshmel, A., *J. Macromol. Sci. B*, 2002, vol. 41, p. 229.
19. Pakhomov, P., Khizhnyak, S., Reuter, H., and Tshmel, A., *J. Appl. Polym. Sci*., 2003, vol. 89, p. 373. doi 10.1002/app.12269
20. Pakhomov, P.M., Golikova, A.Yu., Khizhnyak, S.D., Shavyrina, M.A., Galitsin, V.P., Gribanov, S.A.,

and Kuptsov, S.A., *Fibre Chem.*, 2006, vol. 38, no. 3, p. 200. doi 10.1007/s10692-006-0070-8

21. Galitsyn, V.P., Ro, E.A., Koval', Yu.S., Genis, A.V., Machalaba, N.N., Pakhomov, P.M., Khizhnyak, S.D., Chmel', A.E., and Antipov, E.M., *Fibre Chem.*, 2011, no. 1, p. 33. doi 10.1007/s10692-011-9305-4
22. Pakhomov, P.M., Galitsyn, V.P., Krylov, A.L., Khizhnyak, S.D., Golikova, A.Yu., and Chmel', A.E., *Fibre Chem*, 2005, no. 5, p. 319. doi 10.1007/s10692-006-0002-7
23. Galitsyn, V., Khizhnyak, S., Pakhomov, P., and Tshmel, A., *J. Macromol. Sci. B*, 2003, vol. 42, no. 5, p. 1085.
24. Capaccio, G., Wilding, M.A., and Ward, I.M., *J. Polym. Sci.: Polym. Phys. Ed*., 1981, vol. 19, p. 1489.
25. Tsobkalo, K., Vasilieva, V., Khizhnyak, S., Pakhomov, P., Galitsyn, V., Ruhl, E., Egorov, V., and Tshmel, A., *Polymer*, 2003, vol. 44, no. 5, p. 1613. doi 10.1016/S0032-3861(02)00909-6
26. Dechant, J., Danz, R., Kimmer, W., and Schmolke, R., *Ultrarotspektroskopische untersuchungen an Polymeren*, Berlin: Akademie, 1972.
27. Khizhnyak, S.D., Malanin, M.N., Eichhorn, K.-J., and Pakhomov, P.M., *Polymer Sci., Ser. B*, 2008, vol. 50, no. 6, p. 158. doi 10.1134/S1560090408050138
28. Aulov, V.A. and Kuchkina, I.O., *Polymer Sci., Ser. A*., 2009, vol. 51, no. 8, p. 877. doi 10.1134/S0965545X09080057